Scientia Chromatographica 2014; 6(1):27-33
Instituto Internacional de Cromatografia
http://dx.doi.org/10.4322/sc.2014.017
ISSN 1984-4433

Porous polymer monoliths with incorporated single layer graphene

Lydia Terborg[1]
Simon F. Lux[2]
Michelle Lin[3]
Robert Kostecki[2]
Frantisek Svec[1*]

[1] The Molecular Foundry, E.O. Lawrence Berkeley National Laboratory, Berkeley, CA 94720, USA
[2] Environmental Energy Technologies Division, E.O. Lawrence Berkeley National Laboratory, Berkeley, CA 94720, USA
[3] Department of Chemistry, University of California, Berkeley, CA 94720, USA
*fsvec@lbl.gov

Received: August 22, 2013
Accepted: October 12, 2013

Abstract

Single layer graphene has been used as an additive in poly(butyl methacrylate-*co*-ethylene dimethacrylate) monoliths. Incorporation of the carbon sheets into the polymer matrix was achieved by simple admixing graphene into the polymerization mixture containing both monomers and porogens. Chromatographic experiments indicated that some of the graphene layers were located at the pore surface and increased the apparent hydrophobicity of the material. Raman spectroscopy of the polymer containing graphene documented a rather homogeneous distribution of the single layer graphene sheets over wide areas of the monolith. However, the spectroscopy also confirmed the presence of other areas where the graphene sheets interacted with each other and formed clusters.

Keywords: Monolith; graphene; porous polymer; chromatography; Raman spectroscopy.

1. Introduction

The use of nanomaterials in separation science grew rapidly during the last decade because of their unique characteristics, which have been described in several excellent review articles[1-5]. Carbon-based nanostructures, an important member of the nanomaterials family, have been used in a variety of analytical applications. Nanotubes, fullerenes, nanodiamonds, and graphene have been used in applications such as sample preparation, separations, and detection[6-9]. For example, graphene and its oxidized counterpart were attached to capillary walls or immobilized onto polymer surfaces, and used in micro-extraction, gas chromatography, capillary electrochromatography, and liquid chromatography[10-19].

The unique porous structure of polymer-based monoliths makes them ideally suited for applications which require liquids to rapidly flow through the monolith with only a small amount of pressure, and/or where a fast mass transport is desired. These materials, which were introduced in the early 1990's, are now widely used in rapid chromatographic separations, and as excellent supports for immobilization of catalysts[20-29]. The introduction of carbon nanostructures, (mostly nanotubes and fullerenes), into the field of monoliths was spurred by the quest for improvements in their properties [17,30-33]. The arsenal of carbon nanostructures combined with monoliths was recently extended by the introduction of graphene and its derivatives because of their unique atomic structure, and their interesting electrical, mechanical and chemical properties. For example, Wang and Yan prepared monolithic capillary columns for electrochromatography in a single step by polymerizing a mixture of graphene oxide, methacrylic acid, ethylene dimethacrylate, cyclohexanol, and nitric acid[34]. Tong et al. added graphene nanosheets in a mixture of butyl methacrylate, ethylene dimethacrylate, 1-propanol, 1,4-butanediol, and azobisisobutyronitrile, and then polymerized the mixture in a capillary which produced a device for solid phase extraction of glucocorticoids[35]. Additionally, the same group prepared a poly(glycidyl methacrylate-*co*-ethylene dimethacrylate) monolith in a capillary, modified it with ethylenediamine, and then attached graphene oxide to the free amine functionalities. This monolith was then used for the extraction of sarcosine from urine[36]. Recently, Li et al. reacted graphene oxide with 3-(trimethoxysilyl) propyl methacrylate, and then used the conjugate as a functional crosslinker which was added to a mixture of glycidyl methacrylate and ethylene dimethacrylate. This mixture was polymerized to form a monolithic capillary column designed for the separation of small molecules[37].

A major problem arising from all these approaches is the self-aggregation of the graphene. Due to van der Waals forces and electrostatic interactions, graphene tends to recombine and rebuild layered structures and aggregates from which it originated. Raman spectroscopy is a perfect tool to detect single layer graphene and to characterize the extent of this aggregation since the Raman shift relates directly to the number of graphene layers[38,39].

This communication describes the preparation of porous poly(butyl methacrylate-*co*-ethylene dimethacrylate) monoliths from polymerization mixtures including graphene, and for the first time shows the distribution of single layer and multilayer graphene in the monolith using Raman spectroscopy.

2. Experimental section

2.1. Chemicals and Materials

Monomers, butyl methacrylate and ethylene dimethacrylate, porogenic solvents, 1,4-butanediol and 1-propanol, initiator azobisisobutyronitrile (AIBN), trifluoroacetic acid, 3-(trimethoxysilyl) propyl methacrylate, benzene and ethyl benzene were purchased from Sigma-Aldrich (St. Louis, MO, USA). The monomers were passed through basic aluminum oxide placed in a column to remove the inhibitors. HPLC-grade solvents acetonitrile, acetone, methanol and ethanol were purchased from EMD Chemicals Inc. (Gibbstown, NJ, USA). Single layer graphene powder was purchased from ACS Material LLC (Medford,

MA, USA). All chemicals were of the highest quality available. Polyimide coated 100 μm i.d. fused silica capillaries were purchased from Polymicro Technologies (Phoenix, AZ, USA).

2.2. Preparation of monoliths

The inner surface of the fused silica capillary was "vinylized" with 3-(trimethoxysilyl)propyl methacrylate using a procedure described in detail elsewhere[31] to enable covalent attachment of the monolith. The polymerization mixture for the generic capillary columns consisted of 23.4 wt% 1,4-butanediol and 36.6 wt% 1-propanol, 24.0 wt% butyl methacrylate and 16.0 wt% ethylene dimethacrylate, and AIBN (1 wt% with respect to monomers). In some cases, the single layer graphene powder (0.25 wt% with respect to monomers) was added to the polymerization mixture. The polymerization mixture was homogenized by sonication for 10 min and degassed by purging with nitrogen for 5 min before it was pushed into the vinylized capillary. Both ends of the filled capillary were sealed with a rubber septum, and then the capillary was submerged in a termostated water bath. After completion of the polymerization at 70 °C for 24 h, a piece was cut from both ends of the capillary, the monolith was flushed with acetonitrile to remove the unreacted components, and characterized. The remaining polymerization mixture was polymerized in a glass vial at 70 °C for 24 h, to obtain the bulk material. This monolith was purified with methanol using a Soxhlet extractor and dried in a vacuum oven.

2.3. Instrumentation

Scanning electron micrographs were obtained using a Zeiss Gemini Ultra Field-Emission Scanning Electron Microscope (Peabody, MA, USA). The samples were sputtered with gold using the SCD 050 sputter coater (BAL-TEC AG, Balzers, Lichtenstein). Raman spectra and maps were obtained using a confocal LabRAM Raman microscope from Horiba Jobin Yvon (Edison, NJ, USA). A 1200 series nano flow HPLC system from Agilent Technologies (Santa Clara, CA, USA) consisting of a degasser, a 80 nL UV detection flow cell, and an external microvalve injector with a 10 nL sample loop (Valco Instruments Co Inc., Schenkon, Switzerland) were used for the chromatographic tests. Separation of acetone, benzene, and ethyl benzene was carried out at a flow rate of 2 μL/min using the mobile phase consisting of water and acetonitrile (50/50, v/v). The injection volume was 10 nL and the detection wavelength 210 nm.

3. Results and discussion

3.1. Preparation of methacrylate monoliths containing graphene

The preparation of monolithic columns using butyl methacrylate and ethylene dimethacrylate as monomers has previously been optimized and reported by our group[40]. In the subject experiments we applied this approach to the preparation of monoliths containing graphene. To do so, we first chose to admix the commercial single layer graphene directly into the monomer mixture. To our disappointment, we observed the aggregation of graphene and the formation of a rapidly sedimenting black powder when we added the pristine powder to the mixture containing only both monomers. This result was most likely caused by the highly hydrophobic nature of the graphene itself and its tendency to reform back to the original graphite structure. However, the presence of porogenic solvents, 1-propanol and 1,4-butandiol, in the solution prevented the precipitation. These solvents appear to act as a surfactant and the more protic environment decreases the tendency of graphene to self-aggregate. Vigorous mixing and sonication led to a stable homogeneous black dispersion.

Figure 1 compares SEM images of the original poly(butyl methacrylate-*co*-ethylene dimethacrylate) monolith and its counterpart containing 0.25 wt% graphene, which was the maximum that could be homogeneously dispersed. The polymerization in the presence of the graphene produced a monolith with a changed morphology, and leads to an increase in the size of the through pores. The significant difference in the polymer surface and the dramatically changed structure was clearly visible in images obtained using a larger magnification.

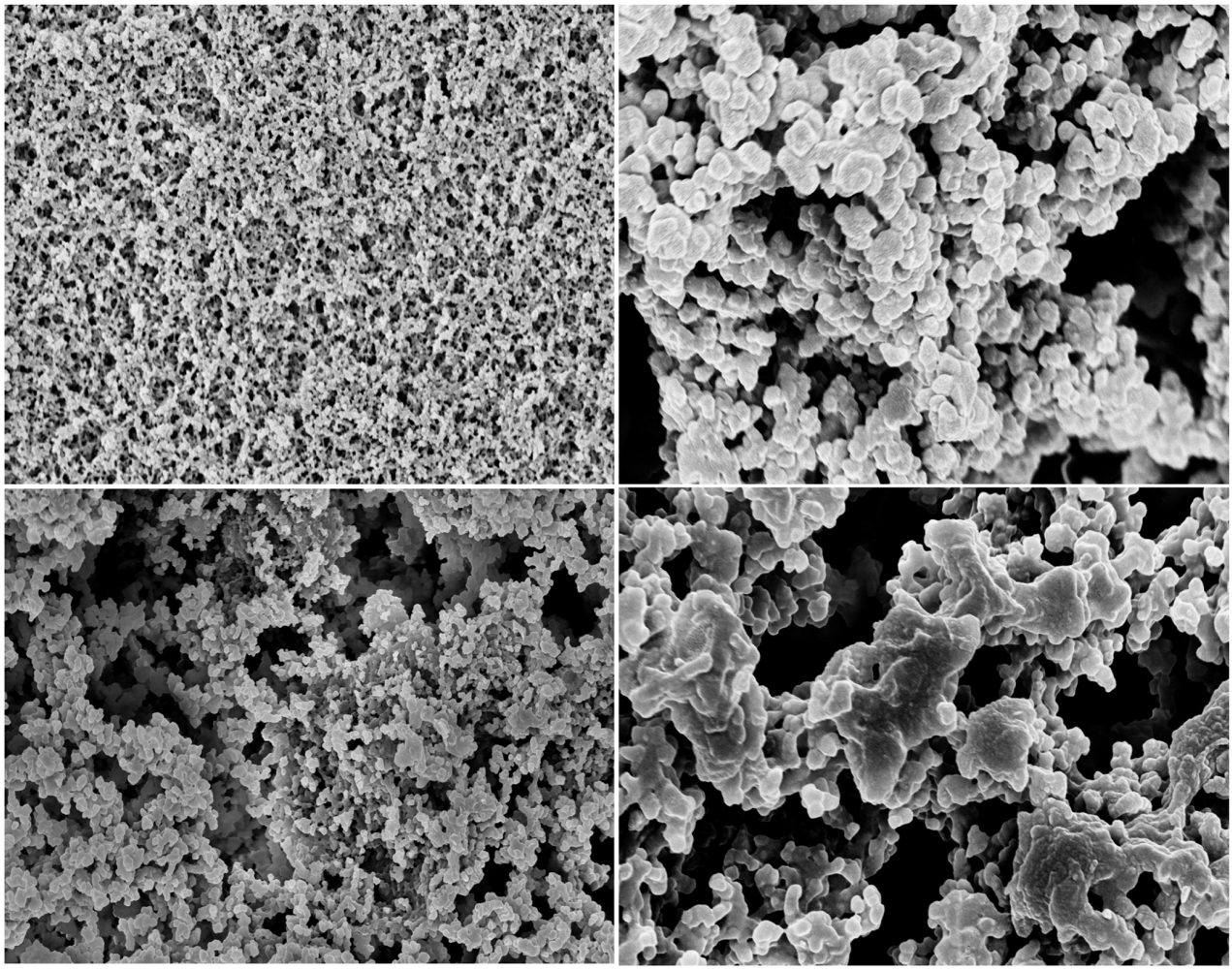

Figure 1. SEM images of poly(butyl methacrylate-*co*-ethylene dimethacrylate)monolith (top) and its counterpart prepared from a polymerization mixture containing 0.25 wt% graphene flakes (bottom).

Interestingly, this change in morphology was not reflected in the changes in surface area of the monoliths. Both the white-colored poly(butyl methacrylate-*co*-ethylene dimethacrylate) monolith and the grayish monolith containing graphene had surface areas of 14 m^2/g. We speculate that this resulted from the small amount of graphene that was added, which even under the best scenario, was not attached perpendicularly to the pore surface. Instead, laied flat and covered the pore surface. As a result, the graphene did not contribute to any increase in the surface area.

Chromatographic experiments provided another piece of evidence indicating the presence of graphene at the pore surface. We used both parent poly(butyl methacrylate-*co*-ethylene dimethacrylate) monolithic capillary columns and its graphene-containing counterpart to separate a mixture of acetone, benzene and ethyl benzene in reversed phase mode. The resulting chromatograms are presented in Figure 2. No separation was achieved using the parent column and only a single broad peak was obtained. In contrast, the presence of a very small amount of graphene increased retention of hydrophobic benzene derivatives and enabled separation of all three compounds. The column efficiency was not very high due to the very small surface area. However, this result clearly indicates that at least part of the graphene was located at the pore surface.

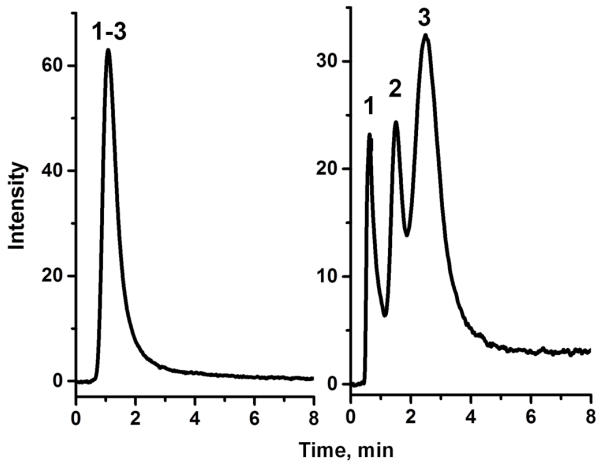

Figure 2. Separation of acetone (1), benzene (2) and ethyl benzene (3) using monolithic poly(butyl methacrylate-*co*-ethylene dimethacrylate) capillary column (A) and its counterpart containing 0.25 wt% (B) entrapped graphene flakes Conditions: Column 10 cm x 100 µm i.d., mobile phase 50:50 vol% acetonitrile- water, flow rate 2.0 µL/min, injection volume 10 nL, UV detection at 210 nm.

3.2. Raman spectroscopy

While the incorporation and possible re-arrangement of the graphene layers into clusters with a graphite-like structure is likely, direct evidence is needed to describe the distribution of the carbonaceous compounds within the monolith. Raman spectroscopy is a simple standard technique for the characterization of sp^2 and sp^3 hybridized carbon atoms in different forms of carbon such as fullerene, graphite, and graphene[38]. In this work Raman spectroscopy was used to investigate the distribution of graphene in both the monoliths prepared in bulk, and in the capillary columns.

First, an argon laser was used with an excitation wavelength of 488 nm that provided spectra with a good resolution. However, the significant background photoluminescence made their interpretation difficult. Therefore, a 532 nm laser was subsequently used to obtain maps with good spatial information. Unfortunately, a broad peak originating from the monolith was present in the range around 2700 cm^{-1}, which was also characteristic for the *2D* peak of graphite and graphene. Therefore, we had to utilize the *G* peak to identify the distribution of graphene in the monolith. Wang et al. found that the wavenumber of the *G* peak for graphene and graphite depends on the number of their layers and shifts toward lower wavenumbers with the increase in the number of layers[41]. The spectrum of the monolithic column containing graphene (shown in Figure 3) exhibits a small split in the *G* peak, most likely representing self-ordering of the graphene layers during or after the preparation of the monolith.

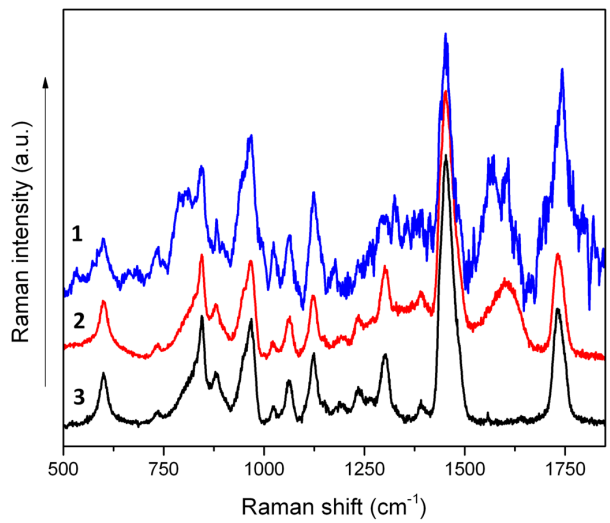

Figure 3. Raman spectra of the bulk monolithic material (3), bulk monolithic material with incorporated graphene (2), and monolith containing graphene in capillary (1).

The excitation wavelength of 532 nm was first utilized to find locations of the *G* peaks for commercial graphite and graphene flakes. The Raman shifts occurred at 1577 cm^{-1} and 1604 cm^{-1}, respectively, and were used to map the distribution of the graphene in the bulk sample. Spectra for the map in Figure 4 were taken every 2 µm and the peak intensity in the different regions was integrated. The white color intensity in the left map refers to the disordered region, which contained the multi-layer graphene or graphite. The map on the right indicates the distribution of graphene which was present in a single-layer or clusters of only a few layers. The images indicate that some of the originally single layer graphene flakes partially reordered during the preparation of the monolithic structure. This process resulted in formation

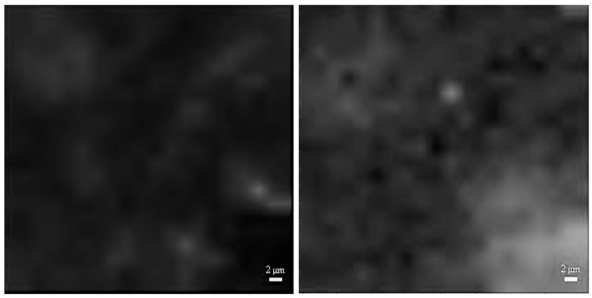

Figure 4. Raman map depicting the distribution of graphene and graphite obtained from the G-band. White color corresponds to the peak intensity 1570-1585 cm^{-1}, i.e. the graphite region (left) and between 1590-1615 cm^{-1} characterizing the graphene region (right).

of disordered regions where graphene layers were located at a distance allowing their interactions with each other. However, and more importantly, this spectral study also confirmed that the graphene monoliths retained a significant amount of graphene in the single layer form since more white spots were seen in the right panel than in the left one.

4. Conclusion

This study demonstrated that poly(butyl methacrylate-*co*-ethylene dimethacrylate) monoliths can be successfully doped/modified with single layer of graphene by its inclusion in the complete polymerization mixture. A significant proportion of the graphene appeared to be incorporated in the polymeric structure in the form of single layers. The increase in hydrophobic interactions indicates that at least a part of graphene was located at the pore surface. Further work will focus on the preparation of monoliths with a greater percentage of graphene and its homogeneous distribution in the polymer. In order to improve the chromatographic performance, monolithic columns with much larger surface areas will be prepared with their surface area increased using the hypercrosslinking reaction.

Acknowledgement

All work presented in this paper was performed at the Molecular Foundry, Lawrence Berkeley National Laboratory and supported by the Office of Science, Office of Basic Energy Sciences, Scientific User Facilities Division of the U.S. Department of Energy, under Contract No. DE-AC02-05CH11231.

References

1. A.S. de Dios and M.E. Diaz-Garcia, *Anal. Chim. Acta,* **666**, 1-22 (2010).
2. C. Nilsson and S. Nilsson, *Electrophoresis,* **27**, 76-83 (2006).
3. C. Nilsson, S. Birnbaum and S. Nilsson, *J. Chromatogr. A,* **1168**, 212-224 (2007).
4. D. Sykora, V. Kasicka, I. Miksik, P. Rezanka, K. Zaruba, P. Matejka and V. Kral, *J. Sep. Sci.,* **33**, 372-387 (2010).
5. Z.X. Zhang, Z.Y. Wang, Y.P. Liao and H.W. Liu, *J. Sep. Sci.,* **29**, 1872-1878 (2006).
6. Q. Liu, J. Shi and G. Jiang, *TrAC Trends Anal. Chem.,* **37**, 1-11 (2012).
7. K. Scida, P.W. Stege, G. Haby, G.A. Messina and C.D. Garcia, *Anal. Chim. Acta,* **691**, 6-17 (2011).
8. A. Speltini, D. Merli and A. Profumo, *Anal. Chim. Acta,* **783**, 1-16 (2013).
9. M. Valcarcel, S. Cardenas and B.M. Simonet, *Anal. Chem.,* **79**, 4788-4797 (2007).
10. J.M. Chen, J. Zou, J.B. Zeng, X.H. Song, J.J. Ji, Y.R. Wang, J. Ha and X. Chen, *Anal. Chim. Acta,* **678**, 44-49 (2010).
11. X. Liu, X. Liu, M. Li, L. Guo and L. Yang, *J. Chromatogr. A,* **1277**, 93-97 (2013).
12. Q. Qu, Y. Shen, C. Gu, Z. Gu, Q. Gu, C. Wang and X. Hu, *Anal. Chim. Acta,* **757**, 83-87 (2012).
13. Q. Qu, C. Gu and X. Hu, *Anal. Chem.,* **84**, 8880-8890 (2012).
14. C. Wang, R.S. de, C.F. Lu, V. Fernand, L. Moore, Jr., P. Berton and I.M. Warner, *Electrophoresis,* **34**, 1197-1202 (2013).
15. L.L. Xu, J.J. Feng, X.J. Liang, J.B. Li and S.X. Jiang, *J. Sep. Sci.,* **35**, 1531-1537 (2012).
16. L.L. Xu, J.J. Feng, J.B. Li, X. Liu and S.X. Jiang, *J. Sep. Sci.,* **35**, 93-100 (2012).
17. Y.Y. Xu, X.Y. Niu, Y.L. Dong, H.G. Zhang, X. Li, H.L. Chen and X.G. Chen, *J. Chromatogr. A,* **1284**, 180-187 (2013).
18. H. Zhang, W.P. Low and H.K. Lee, *J. Chromatogr. A,* **1233**, 16-21 (2012).
19. S.L. Zhang, Z. Du and G.K. Li, *Anal. Chem.,* **83**, 7531-7541 (2011).
20. R.D. Arrua, M. Talebi, T.J. Causon and E.F. Hilder, *Anal. Chim. Acta,* **738**, 1-12 (2012).
21. R. Bakry, C.W. Huck and G.K. Bonn, *J. Chromatogr. Sci.,* **47**, 418-431 (2009).
22. M.R. Buchmeiser, *Polymer,* **48**, 2187-2198 (2007).
23. G. Guiochon, *J. Chromatogr. A,* **1168**, 101-168 (2007).
24. A. Jungbauer and R. Hahn, *J. Chromatogr. A,* **1184**, 62-79 (2008).
25. J. Krenkova, F. Foret and F. Svec, *J. Sep. Sci.,* **35**, 1266-1283 (2012).
26. I. Nischang, *J. Chromatogr. A,* **1287**, 39-58 (2013).
27. I. Nischang, I. Teasdale and O. Bruggemann, *J. Chromatogr. A,* **1217**, 7514-7522 (2010).
28. F. Svec, T.B. Tennikova, Z. Deyl (eds.), *Monolithic Materials: Preparation, Properties, and Applications*, Elsevier, Amsterdam, (2003).
29. F. Svec and C.G. Huber, *Anal. Chem.,* **78**, 2101-2107 (2006).
30. S.D. Chambers, T.W. Holcombe, F. Svec and J.M.J. Fréchet, *Anal. Chem.,* **83**, 9478-9484 (2011).
31. S.D. Chambers, F. Svec and J.M.J. Fréchet, *J. Chromatogr. A,* **1218**, 2546-2552 (2011).
32. Y. Li, Y. Chen, R. Xiang, D. Ciuparu, L.D. Pfefferle, C. Horvath and J.A. Wilkins, *Anal. Chem.,* **77**, 1398-1406 (2005).
33. Y. Zhong, W. Zhou, P. Zhang and Y. Zhu, *Talanta,* **82**, 1439-1447 (2010).
34. M.M. Wang and X.P. Yan, *Anal. Chem.,* **84**, 39-44 (2012).
35. S. Tong, Q. Liu, Y. Li, W. Zhou, Q. Jia and T. Duan, *J. Chromatogr. A,* **1253**, 22-31 (2012).
36. S. Tong, X. Zhou, C. Zhou, Y. Li, W. Li, W. Zhou and Q. Jia, *Analyst,* **138**, 1549-1557 (2013).
37. Y. Li, L. Qi and H. Ma, *Analyst,* **138**, 5470-5478 (2013).
38. A.C. Ferrari, *Solid State Com.,* **143**, 47-57 (2007).
39. P. Lian, X. Zhu, S. Liang, Z. Li, W. Yang and H. Wang, *Electrochimica Acta,* **55**, 3909-3914 (2010).
40. S. Eeltink, L. Geiser, F. Svec and J.M. Fréchet, *J. Sep. Sci.,* **30**, 2814-2820 (2007).
41. H. Wang, Y. Wang, X. Cao, M. Feng and G. Lan, *J. Raman Spectr.,* **40**, 1791-1796 (2009).